Supplemental Figure 1

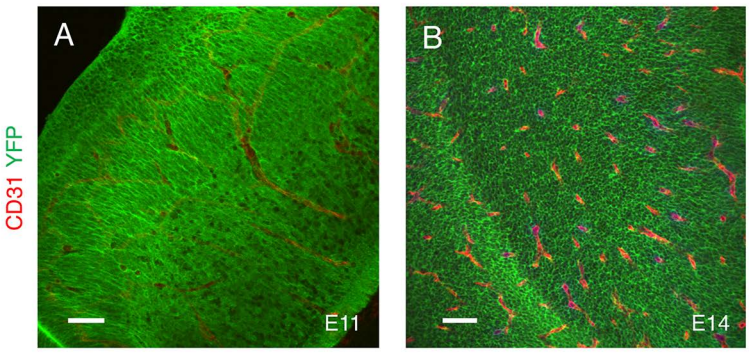

Fig. S1. Analysis of Nestin-Cre-mediated recombination in embryonic brain neuroepithelial cells. (A, B); The Nestin-Cre transgene is expressed in embryonic neuroepithelial cells, but is not expressed in brain blood vessels at E11 (A) and E14 (B) as revealed by the crossing with the Rosa26-loxSTOPlox-YFP reporter model.

Fig. S2. DNA sequencing confirms cytoplasmic domain deletion in cultured mouse Nestin-Cre;ConKO/+ cells. (A); Cre-mediated recombination of the engineered Itgb8 locus removes the mini-gene (Ex13/14), resulting in a premature STOP codon that truncates the β8 integrin protein after the transmembrane domain. **(B, C);** Sanger sequencing of cDNA from E14 Nestin-Cre control and Nestin-Cre;ConKO/+ neurospheres confirmed selective ablation of the β8 integrin cytoplasmic tail coding sequence in Nestin-Cre;ConKO/+ neural progenitor cells. DNA sequences of the ConKI control (B) and ConKO mutant (C) Itgb8 allele confirms Cre-mediated deletion of the Ex13/14 mini-gene and expression of the truncated β8 integrin protein lacking the cytoplasmic signaling domain. The transmembrane sequence is indicated by the red line, and the cytoplasmic domain is indicated by the blue shaded region. The endogenous STOP codon in (B) and the engineered STOP codon in (C) are indicated by red asterisks.

Supplemental Figure 3

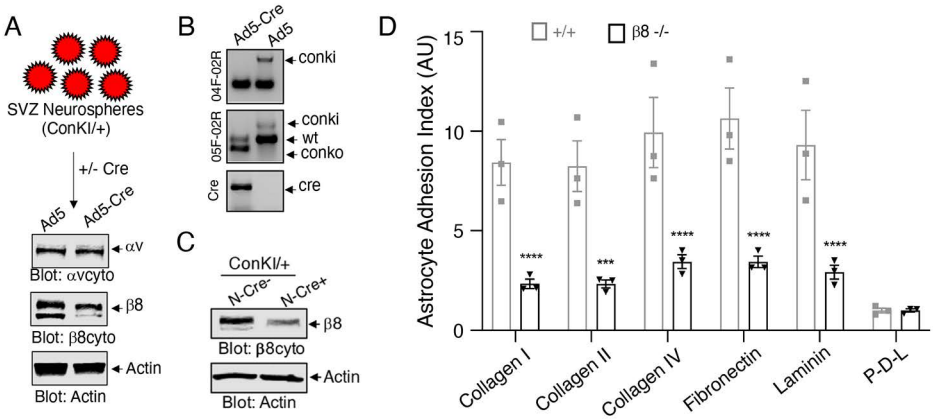

Fig. S3. In vitro validation of Cre-mediated Itgb8 mini-gene deletion and quantitation of β8 integrin ECM adhesion. (A, B); Neurospheres cultured from the subventricular zone of the lateral ventricles of P60 ConKI/+ mice were infected with empty adenovirus (Ad5 control) or adenovirus-Cre (Ad5-Cre). Detergent-soluble lysates were analyzed by immunoblotting with anti-αvcyto or anti-β8cyto integrin antibodies (see Figure 2A). Note the reduction in β8 integrin protein due to truncation of the cytoplasmic domain. Alternatively, Cre-mediated deletion of the floxed mini-gene in the engineered Itgb8 locus was confirmed by genomic PCR (B). **(C);** Neurospheres from E14 control (ConKI/+) or Nestin-Cre;ConKO/+ P0 mice were analyzed by immunoblotting. Note the reduce expression of full-length β8 integrin protein in the neurosphere samples from Nestin-Cre;ConKO/+ embryos. **(D);** Wild type control or β8-/- astrocytes were added to tissue culture wells coated with the indicated ECM proteins and cell adhesion was quantified after 2 hours. Note that β8-/- astrocytes show severe ECM adhesion defects similar to the defects with N-Cre;ConKO/+ astrocytes (Figure 2C). Differences between groups were analyzed using two-way ANOVA and Tukey post-hoc analysis (n=3, mean ± SEM, ***p<0.001, ****p<0.0001).

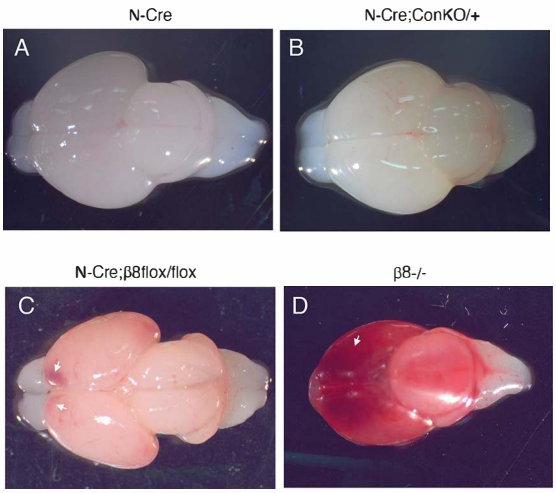

Fig. S4. Lack of intracerebral hemorrhage in Nestin-Cre;ConKO embryos. (A-D); Images of isolated brains from an E18 control (A), Nestin-Cre;ConKO/+ (B), Nestin-Cre;β8flox/flox (C) and β8-/- embryo (D). Note the absence of grossly obvious hemorrhage in the Nestin-Cre;ConKO/+ brains that is less severe than the hemorrhage in the Nestin-Cre;β8flox/flox and β8-/- mutants.

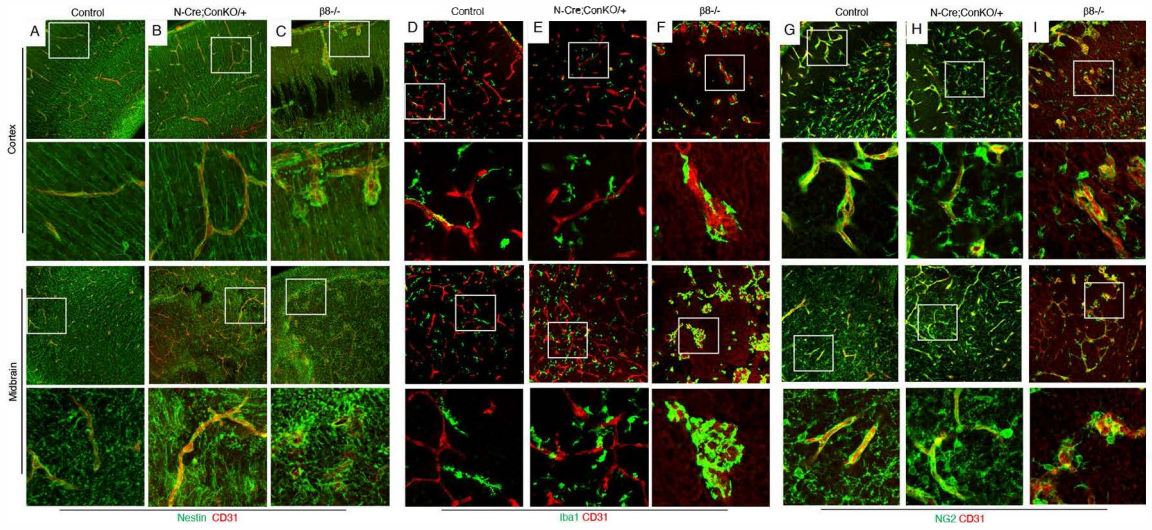

Fig. S5. Neurovascular pathologies in the E18 Nestin-Cre;ConKO/+ brain. (A-C); Sagittal sections through forebrain/neocortical regions or midbrain regions of E18 Nestin-Cre control (A), Nestin-Cre;ConKO/+ (B), or β8-/- embryos (C) were analyzed by double immunofluorescence using anti-CD31 antibodies to detect vascular endothelial cells combined with anti-Nestin to detect neuroepithelial cells. **(D-F);** Sagittal sections through the forebrains/neocortical regions of E18 Nestin-Cre control (D), Nestin-Cre;ConKO/+ (E), or β8-/- embryos (F) were analyzed by double immunofluorescence using anti-CD31 antibodies to detect vascular endothelial cells combined with anti-Iba1 to detect microglial cells. (G-I); Sagittal sections through the forebrains/ neocortical regions of E18 Nestin-Cre control (G), Nestin-Cre;ConKO/+ (H), or β8/- embryos (I) were analyzed by double immunofluorescence using anti-CD31 antibodies to detect vascular endothelial cells combined with anti-NG2 to detect vascular pericytes.

Supplemental Figure 6

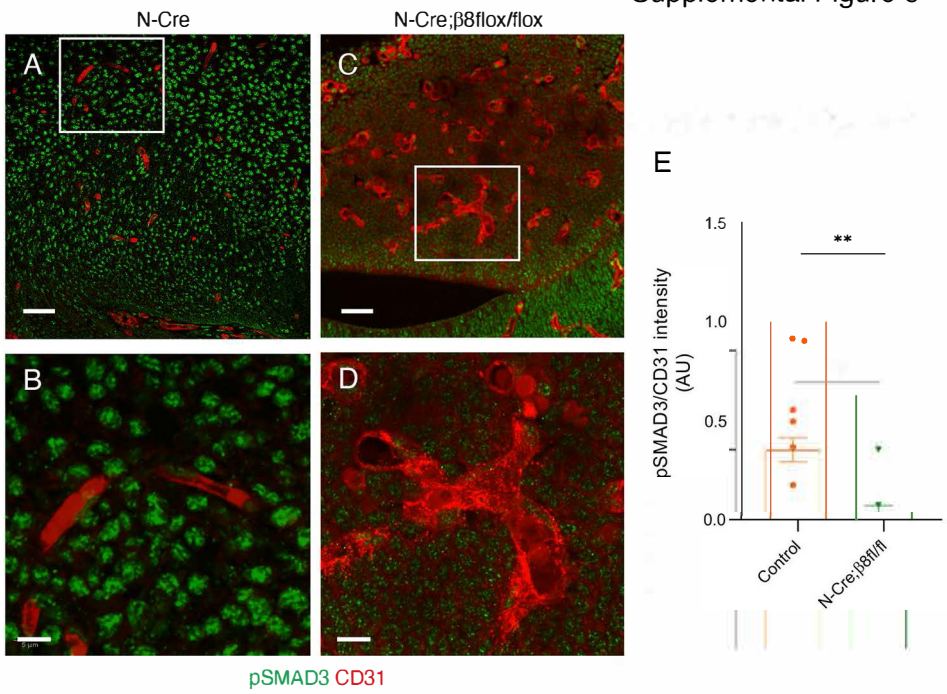

Fig. S6. Conditional knockout of β8 integrin in brain neuroepithelial cells leads to reduced canonical TGFβ receptor signaling in vascular endothelial cells. (A-D); Analysis of Smad3 phosphorylation in sagittal brain sections through telencephalic regions of E14 N-Cre control (A, B) and N-Cre;β8flox/flox embryos (C, D). Note the abnormal CD31^{+} blood vessel morphologies in N-Cre;β8flox/flox brains, with reduced levels of pSmad3. The lower panels are higher magnification images of the boxed areas in the upper panels. (E): Quantification of pSmad3 levels in E14 Nestin-Cre control and Nestin-Cre;β8flox/flox mutant midbrain regions as determined by the bar graph measuring fluorescence intensity of pSmad3 relative to CD31

Supplemental Figure 7

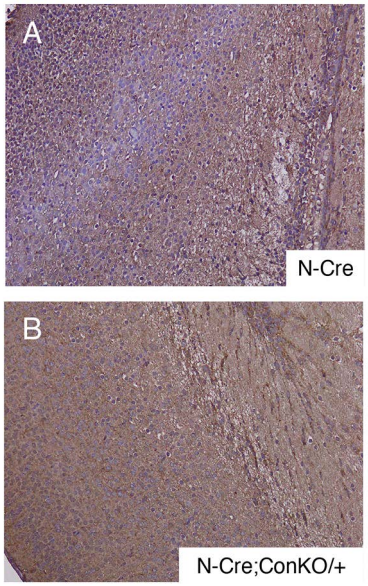

Fig. S7. Analysis of collagen VI protein expression in Nestin-Cre control and Nestin-Cre;ConKO/+ P0 brain sections. (A, B); Formalin fixed and paraffin embedded control (A) and mutant (B) sagittal brain sections were labeled with an anti-Collagen VI antibody. Note the increased levels of Collagen VI expression in the Nestin-Cre;ConKO/+ cortex, versus the control cortex.

Supplemental Figure 8

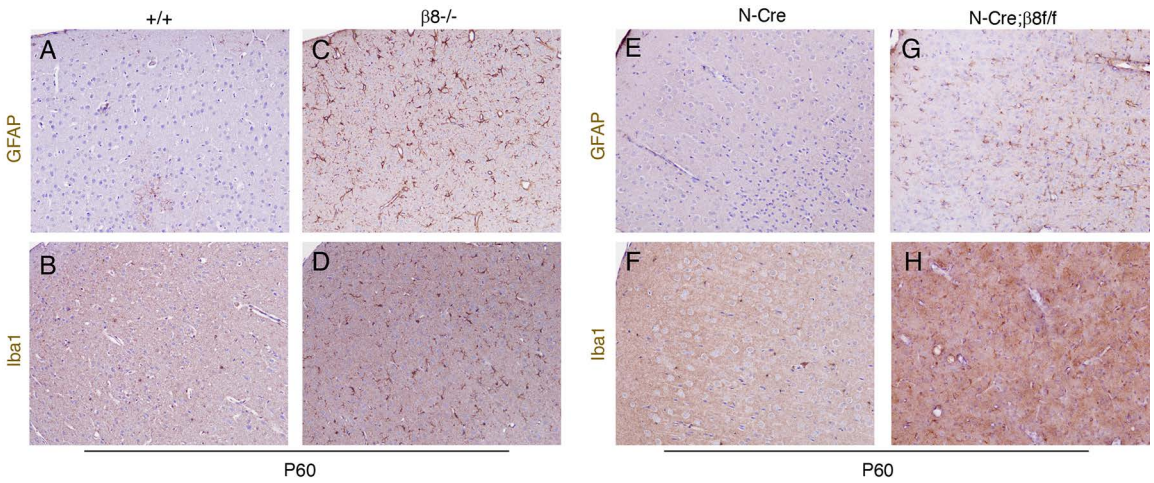

Fig. S8. Brain vascular pathologies in β8-/- and Nestin-Cre;β8flox/flox adult mice. (A-D); Coronal brain sections through the cerebral cortices of wild type control (A, B) or β8-/- (C, D) P60 mice were immunohistochemically labeled with anti-GFAP (A, C) and anti-Iba1 (B, D) antibodies to visualize astrocytes and microglia, respectively. **(E-H);** Coronal brain sections through the cerebral cortices of Nestin-Cre control (E, F) or Nestin-Cre;β8flox/flox (G, H) P60 mice were immunohistochemically labeled with anti-GFAP (E, G) and anti-Iba1 (F, H) antibodies to visualize astrocytes and microglia, respectively. In comparison to control brain sections, note the obvious perivascular Iba1$^+$ microgliosis and GFAP$^+$ astrogliosis in mutant brain sections.

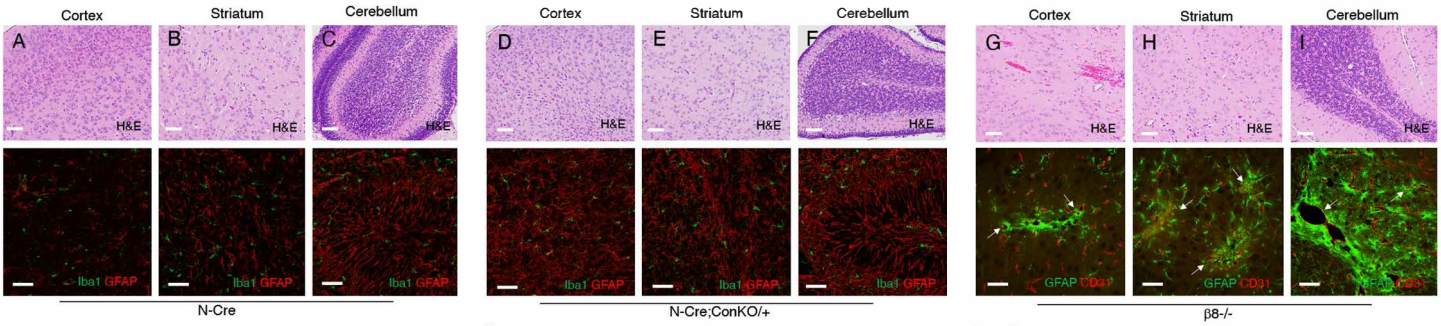

Fig. S9. Microscopic analysis of brains from Nestin-Cre control and Nestin-Cre;ConKO/+ neonatal mice at P10. (A-F); Sagittal brain sections from P10 Nestin-Cre control (A-C) or Nestin-Cre;ConKO/+ mutant mice (D-F) through the cerebral cortex (A, D), striatum (B, E), and cerebellum (C, F) were fixed, paraffin embedded and stained with H&E (upper panels). Alternatively, P10 brains were sectioned with a vibratome and fluorescently labeled with anti-Iba-1 (green) and anti-GFAP (red) antibodies to reveal microglia and astrocytes, respectively. Note the astrogliosis in Nestin-Cre;ConKO/+ mutant brain sections, whereas there is an obvious lack in microgliosis. (D-F). **(G-I);** Sagittal brain sections from P16 β8-/- mutant mice through the cerebral cortex (G), striatum (H), and cerebellum (I) were fixed, paraffin embedded and stained with H&E (upper panels). Alternatively, paraffin embedded brain sections were fluorescently labeled with anti-GFAP (green) and anti-CD31 (red) antibodies to reveal astrocytes and endothelial cells, respectively. Note the microscopic hemorrhage in the cortex (G) as well as robust astrogliosis throughout the β8-/- brain.

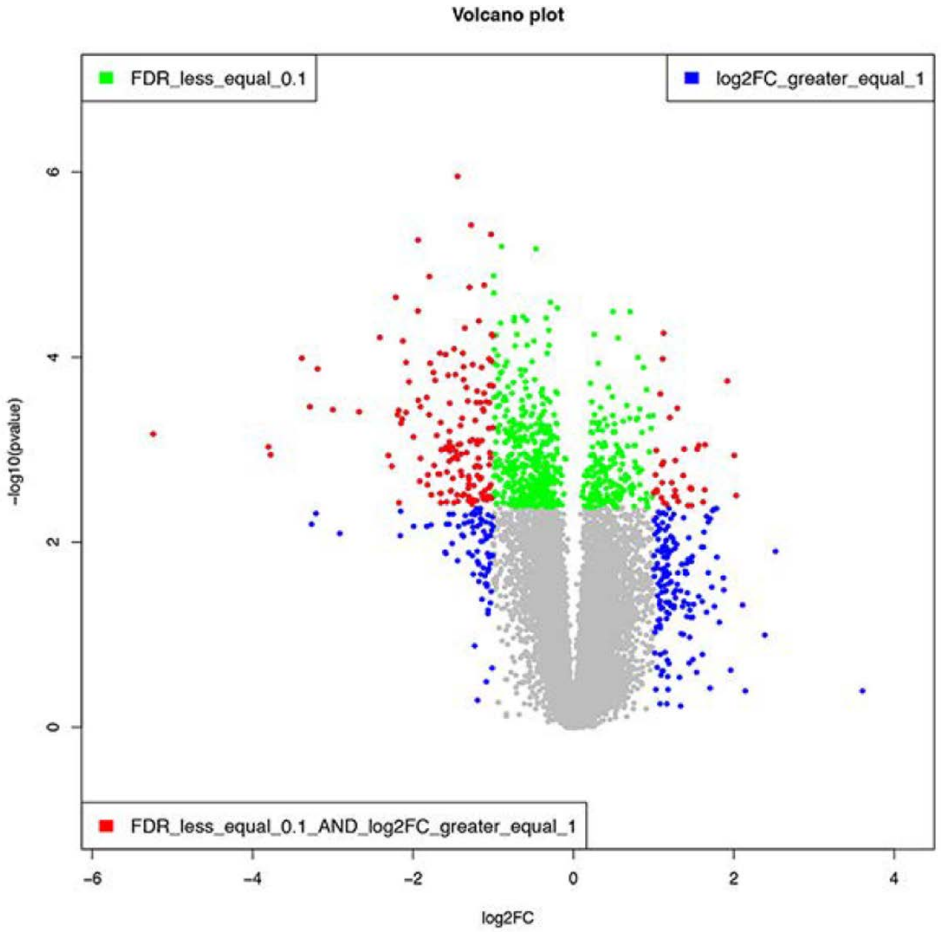

Fig. S10. Volcano plot showing mRNAs in brain endothelial cells that are upregulated and downregulated after Tgfbr2 gene ablation. Quantitative RNA sequencing comparisons reveal differentially expressed genes in PDGFBB-CreERT2f/+ or PDGFBB-CreERT2;Tgfbr2f/f brain endothelial cells isolated from P7 mice as revealed by a color-coded volcano plot. Red indicates higher mRNA expression levels and blue indicates lower expression. Differentially expressed genes were identified using the EdgeR package with adjusted p-value cutoffs <0.05 and log2 fold changes > 2.

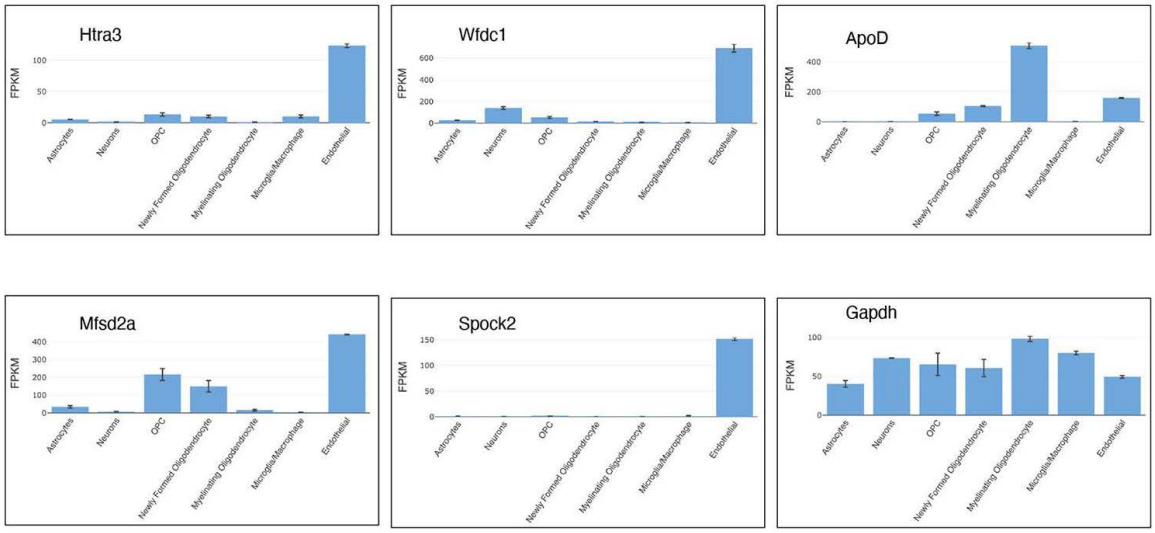

Fig. S11. Validation of brain endothelial cell expression of Tgfbr2-regulated mRNAs identified by quantitative RNA sequencing. Analysis of the brain RNA-seq database (brainrnaseq.org) confirms that the various genes down-regulated after ablation of Tgfbr2 with PDGFBB-CreERT2 at P7 are expressed mainly in brain endothelial cells. In these experiments brain endothelial cells were isolated from P7 Tie2-GFP mice. Gapdh, which is a more broadly expressed gene, is shown as a relative control.

Table S1. Commercial primary antibodies

Primary Antibody	Host(s)	Dilution/ Concentration	Application	Catalog #	Manufacturer
Nestin	Chicken mAb	1:100	IF	CH23001	Neuromics
Iba1	Rabbit pAb	1:250	IF	019-19741	Fujifilm WPCC
Iba1	Rabbit pAb	1:250	IHC-P	013-27691	Fujifilm WPCC
pSMAD3 (S423+S425)	Rabbit mAb	1:200	IF	ab-52903	Abcam
NG2	Rabbit pAb	1:200	IF	AB5320	Millipore Sigma
CD31	Rat mAb	1:200	IF	553370	BD Biosciences
CD31	Goat pAb	1:250	IHC-F	AF3628	R&D Systems
GFAP	Chicken pAb	1:4000	IHC-F, IF	NBP1-05198	Novus
GFAP	Rabbit pAb	1:500	IHC-F, IF	Z0334	Dako
GFP	Chicken	1:2000	IHC-F, IF	GFP-1020	Aves
GFP	Rabbit	1:1000	IHC-F, IF	ab290	Abcam
Isolectin GS-IB_4-Alexa Fluor™ 488	*G. simplicifolia*	1:500	IF	I21411	ThermoFisher
Laminin	Rabbit pAb	1:100	IHC-P	L9393	Sigma Aldrich
Vav1	Rabbit pAb	1:1000	WB	2502	Cell Signaling Technology
Collagen VI	Rabbit pAb	1:1000	WB	17023-1-AP	Proteintech
β8-cyto	Rabbit pAb	1:3000	WB, IP	Custom-made	Covance
αv-cyto	Rabbit pAb	1:3000	WB, IP	Custom-made	Covance
β8-ex	Rabbit pAb	1:1000-1:3000	WB, IP	Custom-made	Covance
β-actin	Mouse mAb	1:3000	WB	A5441	Sigma Aldrich
α-actinin	Mouse mAb	1:3000	WB	AB18061	Abcam
β-actin	Rabbit pAb	1:1000-1:3000	WB	BS-0061R-TR	Bioss
IgG (control)	Rabbit, rat, chicken, goat	1-5 µg/mL (titred based on application)	WB, IF, IHC-P, IHC-F	AB-105-C, 6-001-A, AB-101-C, AB-108-C	R&D Systems

Table S1. Commercial secondary antibodies:

Secondary Antibody	Host	Dilution	Catalog #	Manufacturer
IRDye® anti-Rabbit 800CW	Goat	1:15,000	926-32211	LI-COR
IRDye® anti-Mouse 680CW	Goat	1:15,000	926-68070	LI-COR
IRDye® anti-Rabbit 800CW	Donkey	1:15,000	926-32213	LI-COR
IRDye® anti-Mouse 680CW	Donkey	1:15,000	926-68072	LI-COR
IRDye® Streptavidin 800CW	na	1:5,000	926-32230	LI-COR
Alexa Flour® 488 anti-Chicken	Donkey	1:500	703-545-155	Jackson ImmunoResearch
Alexa Flour® 488 anti-Rabbit	Donkey	1:500	711-545-152	Jackson ImmunoResearch
Alexa Flour® 594 anti-Rat	Donkey	1:500	712-585-153	Jackson ImmunoResearch
Alexa Flour® 594 anti-Goat	Donkey	1:500	705-585-147	Jackson ImmunoResearch

Table S2. Primers used for quantitative real time PCR

Gene	Primer Sequence (5'-3')
mouse Gapdh	*Forward:* GAATGGGAAGCTTGTCATCAACGG
	Reverse: GTAGACTCCACGACATACTCAGCAC
mouse Tgfbr2	*Forward:* TTAACATGATGTCATGGCCAGCG
	Reverse: AGACTTCATGCGGCTTCTCACAGA
mouse Mfsd2a	*Forward:* CCGGTCCAGGTGAAGAAGGAAC
	Reverse: GCTCGGCCCACAAAAAGGATA
mouse Apod	*Forward:* GAAGCCAAACAGAGCAACG
	Reverse: TGTTTCTGGAGGGAGATAAGGA
mouse Htra3	*Forward:* CTCGGGCTTCATCATGTCAGA
	Reverse: AATCGTGGCAATGTCCGACTT
mouse Spock2	*Forward:* ACTGTGATGACATCGTGGGTT
	Reverse: TCTTCTGGCCTGTCTTTCTGG
mouse Wfdc1	*Forward:* TGTCCCTCAGGCTATGAGTG
	Reverse: AAGTGCCTCTGTTGTCCCTTC